

Enhancing Mass Transport for Synthesizing Single-Walled Carbon Nanotubes via Micro Chemical Vapor Deposition

Qin Zhou and Liwei Lin

Abstract—Miniaturization is introduced as a novel methodology to enhance mass transport in a chemical vapor deposition process. As a result, amorphous carbon formation during the synthesis of single-walled carbon nanotubes (SWNTs) can be deterred. Miniaturization also maintains a laminar flow pattern to ensure a stable growth condition. A system with micrometer-sized reaction chambers has been constructed to experimentally verify this concept. The results show that clean and small-diameter SWNTs with approximately millimeter length can be quickly synthesized using ethylene as the source gas. Similar experimental parameters in a conventional large-scale system failed to produce SWNTs with comparable quality due to catalyst poisoning. [2010-0296]

Index Terms—Carbon nanotube, chemical vapor deposition (CVD), microelectromechanical system.

Chemical vapor deposition (CVD) has been broadly adopted to grow single-walled carbon nanotubes (SWNTs) [1], [2]. However, it has been well documented that this growth process will terminate after a short period of time (usually several minutes) [2], [3]. The reason, as suspected by many groups, is the formation of amorphous carbon [4]–[7] that poisons the catalyst nanoparticles. The generally established growth mechanism for SWNTs is the vapor–liquid–solid (VLS) process [7]–[10] in which carbon from the decomposed hydrocarbon gas is absorbed by nanoparticle catalysts at a high temperature, and SWNTs are grown as a result of carbon supersaturation. The formation of amorphous carbon, on the other hand, does not require catalysts and is therefore a direct vapor–solid (VS) process. Various methods and carefully chosen experimental parameters have been implemented [11], [12] to inhibit this process, resulting in nanotubes of millimeter length and free of amorphous carbon. Most of these methods are chemical, using different gas sources or catalysts. One example is to introduce hydrogen gas into the system, thereby impeding the forward progress of the decomposition reaction of hydrocarbon gas, as suggested by Le Chatelier’s principle [4]. However, this method would also suppress carbon supersaturation and, therefore, the growth of SWNTs. A novel physical method is thus introduced in this paper.

The different growth mechanisms between SWNTs (VLS process) and amorphous carbon (VS process) provide the possibility of promoting one process and suppressing the other. This could be accomplished via “enhanced mass transport” by increasing the rate of gas molecules entering and leaving reaction sites during the growth process. Slower mass transport allows the gas to remain in the immediate vicinity of the reaction site at a high temperature for a longer period of time, increasing the likelihood of decomposition [13]. As a result, promoting mass transport could suppress the formation of amorphous carbon while having no effect on the SWNT growth since the process is usually limited by the reaction rate rather than mass transport [14].

Manuscript received October 14, 2010; revised November 10, 2010; accepted November 17, 2010. Date of publication January 6, 2011; date of current version February 2, 2011. Subject Editor C. Liu.

The authors are with the Berkeley Sensor and Actuator Center, University of California, Berkeley, CA 94720-1774 USA (e-mail: zhouqin1983@gmail.com; lwlin@me.berkeley.edu).

Color versions of one or more of the figures in this paper are available online at <http://ieeexplore.ieee.org>.

Digital Object Identifier 10.1109/JMEMS.2010.2100035

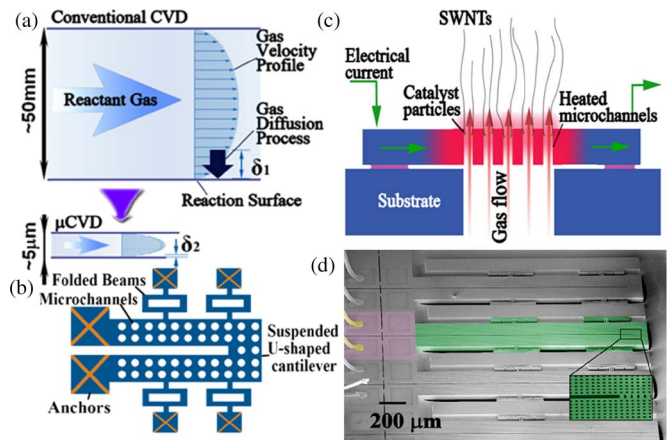


Fig. 1. (a) Mass transport of a CVD process can be enhanced by miniaturization which reduces the diffusion length δ . (b) Conceptual top view and (c) cross-sectional view of a μ CVD system constructed by micromachining processes. The suspended U-shaped cantilever is heated by applying electrical current, and the built-in microchannels are used to emulate furnaces in conventional CVD systems. (d) SEM image of a fabricated μ CVD array with several μ CVD units. The colored region indicates one of the units with the electrical wires in yellow color, the bonding pads in purple color, and the U-shaped cantilever in green color where (inset) many vertical microchannels are built in.

The mass transport process can be enhanced by increasing the gas flow rate. In most atmospheric pressure synthesis processes, the gas velocity near the reaction surface is close to zero, as shown in Fig. 1(a). As a result, the reactant gas does not directly impinge on the substrate but diffuses through a distance δ to the reaction surface. The diffusion length δ is the distance from the reaction surface to the convective gas stock, where gas can freely flow in and out. A small δ corresponds to a short distance that the gas has to diffuse through to reach the reaction surface, yielding fast mass transport. One way to reduce δ is to increase the velocity gradient (calculated in the direction perpendicular to the reaction surface) near the reaction surface in which case flow streams with a higher velocity are drawn closer to the reaction surface. A simple way to increase the velocity gradient is to increase the flow rate. However, it has been discovered that, in conventional CVD systems, this could result in turbulent flow and affect the quality of SWNTs [14], [15].

Herein, we propose to simultaneously enhance mass transport and avoid turbulence using the micro-CVD (μ CVD) system, as shown in Fig. 1(a). Analytically, the flow velocity inside a tube with a circular cross section is described by the parabolic velocity profile [16]

$$v(r) = 2v_m \cdot [1 - (r/r_0)^2] \quad (1)$$

where r is the radial coordinate, v_m is the mean gas velocity, and r_0 is the radius of the tube. The velocity gradient near the inner surface of the tube is

$$\left. \frac{\partial v(r)}{\partial r} \right|_{r=r_0} = \frac{4v_m}{r_0} \quad (2)$$

It is noted in (2) that, aside from increasing v_m , the velocity gradient can also be increased by reducing the tube radius, which scales as r_0^{-1} . Specifically, if the microchannel diameter is $5 \mu\text{m}$ as compared to a 50-mm conventional quartz tube, a 10^4 increase in velocity gradient can be achieved under the same mean flow velocity. This large velocity gradient could significantly enhance mass transport.

Maintaining laminar gas flow requires a small Reynolds number [17], which is defined as

$$Re = \frac{\rho v_m D}{\mu} \quad (3)$$

where ρ is the gas density, μ is the gas viscosity, and D is the tube diameter. The Reynolds number could be reduced by about four orders of magnitude if the tube diameter is reduced from a typical 50-mm setup to a microchannel with a 5- μm diameter. As a result, laminar flow can be easily achieved.

The aforementioned discussions for gas flow in μCVD are valid because the flow resides in the continuum flow region. For most SWNT synthesis processes, the mean free path of gas molecules under one atmospheric pressure is on the order of tens of nanometers, which is much smaller than the diameter of the proposed microchannel [18].

Fig. 1(b) and (c) shows the schematic top view and cross-sectional view of the proposed microstructure where a U-shaped cantilever, which contains many vertically positioned microchannels, is used as a localized resistive heating source. Four folded beams acting as supporting springs provide mechanical strength in the vertical direction and can withstand thermal stress during the heating process. A simple two-step deep reactive ion etching process is performed on a silicon-on-insulator wafer to construct the U-shaped heater, the built-in microchannels from the top, and the backside openings from the bottom. The top device layer is boron-doped silicon with a resistivity of $0.001 \Omega \cdot \text{cm}$ and a thickness of $50 \mu\text{m}$. Afterward, a $0.5\text{-}\mu\text{m}$ -thick thermal oxide layer is grown as a barrier layer to prevent catalyst iron nanoparticles from diffusing into the silicon during the SWNT growth. A photolithography step is used to remove oxide on the contact pad area to allow electrical contacts. Iron nanoparticles are then deposited by a solution-based method [19], [20]. Fig. 1(d) shows a scanning electron microscope (SEM) image of a fabricated sample with four μCVD units in an array.

Ethylene and hydrogen (volume ratio 3:20) were used in the experiments. The measured pressure drop from the backside opening underneath the testing chip to the testing chamber is 250 Pa. The pressure drop of an individual microchannel should be close to 250 Pa since the microchannels experience a much larger flow resistance than macro-sized gas lines. The mean flow velocity v_m can therefore be estimated as [16]

$$v_m = \frac{r_0^2}{8\mu L_{mc}} \frac{\Delta p}{L_{mc}} \approx \frac{(2.5 \mu\text{m})^2 \times 250 \text{ Pa}}{8 \times 8.4 \times 10^{-6} \text{ Pa} \cdot \text{s} \times 50 \mu\text{m}} \approx 40 \text{ cm/s} \quad (4)$$

where p is the gas pressure and L_{mc} is the length of the microchannels. The viscosity of hydrogen is used in this calculation. Notice that the applied pressure is much larger than that in a conventional setup (on the order of 10^{-3} Pa for 3000-sccm flow in a 50-mm inner-diameter tube with a 1-m length) to achieve comparable flow velocity.

In the experiments on a prototype μCVD system, an electrical current of 180 mA was used, and the temperature of the tip region (center of the U-shaped heater) reached about 900°C based on a simplified electrothermal model and experimental verification [21]–[23]. It was observed under SEM analyses that dense and long SWNT growth occurred in the regions with a temperature of approximately 800°C . The temperature of the whole U-shaped cantilever was not uniform, but the temperature of a particular microchannel was locally uniform and stable to grow SWNTs.

Fig. 2(a) shows the synthesis results of SWNTs by the μCVD system. In this experiment, in addition to the vertical gas supply through the microchannels, gas was additionally flowed horizontally on the

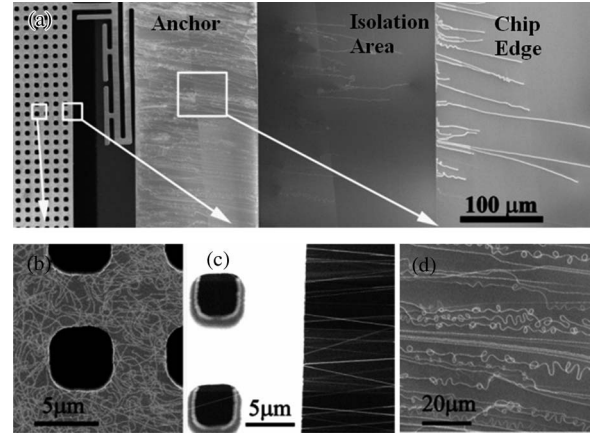


Fig. 2. SEM images showing growth results. (a) Overview. The left side is the growth side, and a portion of the U-shaped microheater is shown. SWNTs fell to the right due to the external horizontal gas flow. (b) Close view near the microchannel region showing randomly distributed SWNTs. (c) High-contrast SEM image close to the edge of the microheater revealing many suspended SWNTs over the through-hole regions. (d) Close view showing longer and aligned SWNTs that are lying on nearby structures.

top surface of the μCVD system from left to right. This flow can force SWNTs to fall rightward onto nearby microstructures after the growth process. As a result, the structures seen in the SEM photograph from left to right are as follows: a region of the μCVD heater with built-in microchannels, a dark through-hole region, a folded beam structure, an anchor for a folded beam, an isolation area (without the top silicon device layer to isolate the individual μCVD systems), and a chip edge shoulder. Some gas will leak from the dark through-hole region during growth. Severe leakage can change the pressure difference across the microchannels significantly and therefore invalidate the previous analysis on gas flow. Fortunately, the width of the slit is only approximately $20 \mu\text{m}$, which is much smaller than gas feeding lines whose diameters are at least several millimeters. As a result, its flow resistance (connected in parallel with the microchannels) is large and will not affect the previous approximation that the measured pressure difference equals the pressure drop between the two sides of a microchannel. The synthesized SWNTs grew up to 0.7 mm in length in a 30-min growth process. In the microchannel area as shown in Fig. 2(b), SWNTs were distributed randomly as they grew and fell onto the substrate. Over the through-hole region, SWNTs were suspended and difficult to distinguish, so a high-contrast SEM photograph was taken to reveal them in Fig. 2(c). Some of the longer SWNTs can be observed in Fig. 2(d) in the anchor region. It is believed that the growth mechanism of these long SWNTs was base growth; otherwise, catalyst particles would be far away from the heat source, and no growth could occur.

The nanotubes synthesized by μCVD were free of amorphous carbon as seen in the close view SEM photograph in Fig. 3(a). Atomic force microscopy (AFM) was used to verify the results in Fig. 3(b). It is found that most synthesized nanotubes were single walled and had diameters in the range of 1–2 nm. They appeared to have larger diameters under SEM due to charge effects [24]. This is the first successful attempt to grow clean and small-diameter SWNTs using the μCVD system with solution-based iron nanoparticles as catalysts and hydrogen and ethylene as gas sources. Methane [2], ethanol [12], or carbon monoxide [25] is usually reported as the carbon source in the growth of SWNTs. Ethylene is sometimes added in very small amounts to increase gas activity [26] but has never been used successfully as the main carbon source, except for the “supergrowth” mechanism [3] where water is added to keep the catalyst active. The difficulty of using ethylene as the main carbon source is that ethylene

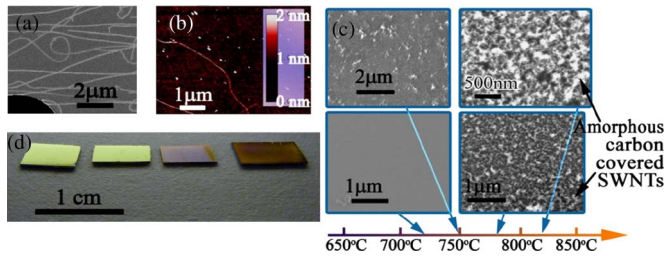


Fig. 3. SWNTs synthesized from μ CVD and conventional CVD. (a) SEM image showing clean SWNTs from μ CVD. (b) AFM image is used to characterize the diameter of SWNTs from μ CVD. (c) SEM photographs showing results from control experiments to synthesize SWNTs from conventional furnace, with the same source gas under different growth temperatures from 720 °C to 820 °C. (d) Optical images of the chips in (c), showing amorphous carbon formation at high temperatures.

decomposition starts at a relatively low temperature (~ 750 °C) while small-diameter SWNT growth usually happens at a higher temperature (> 800 °C) [7]. As a result, amorphous carbon from the pyrolysis of ethylene can easily deposit in large amounts to block the growth of SWNTs.

Control experiments have been conducted using a conventional CVD setup with the same catalyst and gas inputs under various temperatures between 600 °C and 850 °C. It was observed that no growth occurred at low temperatures, and as the growth temperature increased, short and curly nanotubes were grown, but they were covered by a significant amount of amorphous carbon. The SEM photographs of samples grown in 5 min at 720 °C, 750 °C, 780 °C, and 820 °C are shown, respectively, in Fig. 3(c). Optical observation of the 820 °C growth showed a black substance covering all the chips [see Fig. 3(d)] as well as the walls of the growth furnace. The widely spread black substance was considered to be amorphous carbon as its formation does not require catalysts. It is concluded that μ CVD significantly enhances mass transport without causing turbulence and, thus, may allow the use of a wider variety of gas sources for potentially new synthesis results.

REFERENCES

- [1] J. Kong, A. M. Cassell, and H. J. Dai, "Chemical vapor deposition of methane for single-walled carbon nanotubes," *Chem. Phys. Lett.*, vol. 292, no. 4–6, pp. 567–574, Aug. 14, 1998.
- [2] J. Kong, H. T. Soh, A. M. Cassell, C. F. Quate, and H. J. Dai, "Synthesis of individual single-walled carbon nanotubes on patterned silicon wafers," *Nature*, vol. 395, no. 6705, pp. 878–881, Oct. 29, 1998.
- [3] K. Hata, D. N. Futaba, K. Mizuno, T. Namai, M. Yumura, and S. Iijima, "Water-assisted highly efficient synthesis of impurity-free single-walled carbon nanotubes," *Science*, vol. 306, no. 5700, pp. 1362–1364, Nov. 19, 2004.
- [4] N. R. Franklin, Y. M. Li, R. J. Chen, A. Javey, and H. J. Dai, "Patterned growth of single-walled carbon nanotubes on full 4-inch wafers," *Appl. Phys. Lett.*, vol. 79, no. 27, pp. 4571–4573, Dec. 31, 2001.
- [5] D. N. Futaba, K. Hata, T. Yamada, K. Mizuno, M. Yumura, and S. Iijima, "Kinetics of water-assisted single-walled carbon nanotube synthesis revealed by a time-evolution analysis," *Phys. Rev. Lett.*, vol. 95, no. 5, p. 056104, Jul. 29, 2005.
- [6] G. Zhang, D. Mann, L. Zhang, A. Javey, Y. Li, E. Yenilmez, Q. Wang, J. P. McVittie, Y. Nishi, J. Gibbons, and H. Dai, "Ultra-high-yield growth of vertical single-walled carbon nanotubes: Hidden roles of hydrogen and oxygen," *Proc. Nat. Acad. Sci. U.S.A.*, vol. 102, no. 45, pp. 16 141–16 145, Nov. 8, 2005.
- [7] A. R. Harutyunyan, E. Mora, T. Tokune, K. Bolton, A. Rosen, A. Jiang, N. Awasthi, and S. Curtarolo, "Hidden features of the catalyst nanoparticles favorable for single-walled carbon nanotube growth," *Appl. Phys. Lett.*, vol. 90, no. 16, p. 163120, Apr. 16, 2007.
- [8] L. Alvarez, T. Guillard, J. L. Sauvajol, G. Flamant, and D. Laplaze, "Growth mechanisms and diameter evolution of single wall carbon nanotubes," *Chem. Phys. Lett.*, vol. 342, no. 1/2, pp. 7–14, Jul. 6, 2001.
- [9] S. Helveg, C. Lopez-Cartes, J. Sehested, P. L. Hansen, B. S. Clausen, J. R. Rostrup-Nielsen, F. Abild-Pedersen, and J. K. Nørskov, "Atomic-scale imaging of carbon nanofibre growth," *Nature*, vol. 427, no. 6973, pp. 426–429, Jan. 29, 2004.
- [10] J. C. Charlier and S. Iijima, "Growth mechanisms of carbon nanotubes," *Carbon Nanotubes*, vol. 80, pp. 55–81, 2001.
- [11] H. T. Liu, J. He, J. Y. Tang, H. Liu, P. Pang, D. Cao, P. Krstic, S. Joseph, S. Lindsay, and C. Nuckolls, "Translocation of single-stranded DNA through single-walled carbon nanotubes," *Science*, vol. 327, no. 5961, pp. 64–67, Jan. 1, 2010.
- [12] Y. L. Li, I. A. Kinloch, and A. H. Windle, "Direct spinning of carbon nanotube fibers from chemical vapor deposition synthesis," *Science*, vol. 304, no. 5668, pp. 276–278, Apr. 9, 2004.
- [13] J.-H. Park and T. S. Sudarshan, *Chemical Vapor Deposition*. Materials Park, OH: ASM Int., 2001.
- [14] Z. Jin, H. Chu, J. Wang, J. Hong, W. Tan, and Y. Li, "Ultralow feeding gas flow guiding growth of large-scale horizontally aligned single-walled carbon nanotube arrays," *Nano Lett.*, vol. 7, no. 7, pp. 2073–2079, Jul. 2007.
- [15] B. H. Hong, J. Y. Lee, T. Beetz, Y. M. Zhu, P. Kim, and K. S. Kim, "Quasi-continuous growth of ultralong carbon nanotube arrays," *J. Amer. Chem. Soc.*, vol. 127, no. 44, pp. 15 336–15 337, Nov. 9, 2005.
- [16] F. P. Incropera, *Fundamentals of Heat and Mass Transfer*, 6th ed. Hoboken, NJ: Wiley, 2007.
- [17] J. P. Holman, *Heat Transfer*, 9th ed. New York: McGraw-Hill, 2002.
- [18] R. G. Livesey, "Solution methods for gas flow in ducts through the whole pressure regime," *Vacuum*, vol. 76, no. 1, pp. 101–107, Oct. 29, 2004.
- [19] Q. Zhou and L. Lin, "Micro chemical vapor deposition system: Design and verification," in *Proc. 22nd IEEE Int. Conf. Microelectromech. Syst.*, Sorrento, Italy, 2009, pp. 587–590.
- [20] H. C. Choi, S. Kundaria, D. W. Wang, A. Javey, Q. Wang, M. Rolandi, and H. J. Dai, "Efficient formation of iron nanoparticle catalysts on silicon oxide by hydroxylamine for carbon nanotube synthesis and electronics," *Nano Lett.*, vol. 3, no. 2, pp. 157–161, Feb. 2003.
- [21] L. W. Lin and M. Chiao, "Electrothermal responses of lineshape microstructures," *Sens. Actuators A, Phys.*, vol. 55, no. 1, pp. 35–41, Jul. 15, 1996.
- [22] O. Englander, D. Christensen, and L. W. Lin, "Local synthesis of silicon nanowires and carbon nanotubes on microbridges," *Appl. Phys. Lett.*, vol. 82, no. 26, pp. 4797–4799, Jun. 30, 2003.
- [23] S. Li, K. Zhang, J. M. Yang, L. W. Lin, and H. Yang, "Single quantum dots as local temperature markers," *Nano Lett.*, vol. 7, no. 10, pp. 3102–3105, Oct. 2007.
- [24] Y. Homma, S. Suzuki, Y. Kobayashi, M. Nagase, and D. Takagi, "Mechanism of bright selective imaging of single-walled carbon nanotubes on insulators by scanning electron microscopy," *Appl. Phys. Lett.*, vol. 84, no. 10, pp. 1750–1752, Mar. 8, 2004.
- [25] B. Zheng, C. G. Lu, G. Gu, A. Makarovski, G. Finkelstein, and J. Liu, "Efficient CVD growth of single-walled carbon nanotubes on surfaces using carbon monoxide precursor," *Nano Lett.*, vol. 2, no. 8, pp. 895–898, Aug. 2002.
- [26] N. R. Franklin and H. J. Dai, "An enhanced CVD approach to extensive nanotube networks with directionality," *Adv. Mater.*, vol. 12, no. 12, pp. 890–894, Jun. 16, 2000.